Nonlinear ion-acoustic cnoidal waves in a dense relativistic degenerate magnetoplasma

E. F. El-Shamy*

Department of Physics, Faculty of Science, Damietta University, New Damietta 34517, Egypt and Department of Physics, College of Science, King Khalid University, P.O. 9004, Abha, Kingdom of Saudi Arabia

(Received 27 October 2014; published 6 March 2015)

The complex pattern and propagation characteristics of nonlinear periodic ion-acoustic waves, namely, ion-acoustic cnoidal waves, in a dense relativistic degenerate magnetoplasma consisting of relativistic degenerate electrons and nondegenerate cold ions are investigated. By means of the reductive perturbation method and appropriate boundary conditions for nonlinear periodic waves, a nonlinear modified Korteweg–de Vries (KdV) equation is derived and its cnoidal wave is analyzed. The various solutions of nonlinear ion-acoustic cnoidal and solitary waves are presented numerically with the Sagdeev potential approach. The analytical solution and numerical simulation of nonlinear ion-acoustic cnoidal waves of the nonlinear modified KdV equation are studied. Clearly, it is found that the features (amplitude and width) of nonlinear ion-acoustic cnoidal waves are proportional to plasma number density, ion cyclotron frequency, and direction cosines. The numerical results are applied to high density astrophysical situations, such as in superdense white dwarfs. This research will be helpful in understanding the properties of compact astrophysical objects containing cold ions with relativistic degenerate electrons.

DOI: 10.1103/PhysRevE.91.033105 PACS number(s): 52.35.Fp, 52.35.Dm, 52.35.Mw

I. INTRODUCTION

In recent years, there has been enormous interest in the study of new aspects of collective interactions in dense quantum plasmas [1–4]. Quantum plasma physics has a very high particle number density and a low particle temperature, in comparison with classical plasmas where the plasma particle number density is relatively low and the plasma temperature is rather high. Recent evidence suggests that dense quantum plasmas would be used to establish a suitable frame for investigating many astrophysical phenomena in interstellar compact objects. Actually, there are many interstellar compact objects where matters exist in extreme conditions [5–10] not found in terrestrial environments. One of the extreme conditions found in these objects is a high density of degenerate matter. These compact objects are relics of stars which have ceased burning thermonuclear fuel and therefore no longer generate thermal pressure. These interstellar compact objects have significantly contracted, and, as a result, the density of their interiors becomes high enough to provide nonthermal pressure via degenerate fermion/electron pressure and particle-particle interactions. One of the examples of these kinds of stars (i.e., interstellar compact objects) is a white dwarf, which is supported by the pressure of degenerate electrons.

It is established that white dwarf stars have low luminosity and high surface emissivity, with masses typically less than one solar mass and radii typically less than 10^6 solar radius. The average bulk densities of white dwarf stars are typically 10^{30} cm^3. The number density of the degenerate electrons can be order of 10^{30} cm^3 or more in compact objects such as white dwarfs, which is very high [11]. Therefore, one of the most interesting quantum phenomena is the structure of white dwarf stars, which couple the degeneracy of electrons due to the Pauli exclusion principle and Heisenberg's uncertainty principle to the stability of the white dwarf star on macroscopic scales via the balance between the gravitational pull and the degeneracy pressure of the electrons. Mathematically, it is well established that the equation of state for degenerate electrons in such interstellar compact objects was deduced by Chandrasekhar [5–7] for two cases, $P_e \sim n_e^{5/3}$ for the nonrelativistic case and $P_e \sim n_e^{4/3}$ for the ultrarelativistic case, where P_e is the degenerate electron pressure and n_e is the degenerate electron number density. In other words, when the Fermi energy of the electrons becomes comparable to or higher than the electron rest energy, the equation of state changes to $P_e \sim n_e^{4/3}$, which makes the white dwarf star gravitationally unstable for masses larger than about 1.4 solar masses [5–7]. It is well known that the observation of white dwarf stars is mainly due to their electromagnetic radiation, which unravels their physical properties and dynamics [8]. To date, there have been about 200 observations of pulsating white dwarf stars, which fall in the range from 2 to 35 min and can be attributed to nonradial gravity oscillation modes. The observations and theory of these pulsations are employed to investigate the rotation period, mass, as well as equation of state of these stars [12,13]. In addition to the gravity waves, the theory also predicts the existence of acoustic oscillation modes where the ions provide the inertia and mainly the electron degeneracy pressure provides the restoring force. Typical oscillation periods of globally propagating acoustic modes are set by the time for the wave to travel across the star and lie in the range of a few seconds, two orders of magnitude shorter than gravity mode oscillations. These modes were predicted early on [14], but have yet to be observed. The lack of observations, however, does not necessarily imply the absence of acoustic mode oscillations, but may be associated with the motion below the detection limit [15]. The possibility of the formation of finite amplitude acoustic waves is also suggested in the case of extreme events such as supernova explosions and pulsating white dwarf stars [11]. Therefore, our objective here is to develop a nonlinear theory of nonlinear periodic ion-acoustic waves (i.e., ion-acoustic cnoidal waves), in a dense magnetoplasma with relativistic degenerate electrons.

Nowadays, increasing interest in the study of nonlinear periodic waves in plasmas as well as in other dispersive media

*emadel_shamy@hotmail.com

has become important due to their application in diverse areas of physics such as the nonlinear transport phenomenon. Before giving an outline of this article, it is useful to define cnoidal waves. Indeed, cnoidal waves based on Jacobian elliptical functions, such as sn, cn, and dn waves, are exact solutions in the form of periodic pulses. One of the most important features of cnoidal waves is that, in the limit of strong spatial localization, they transform into well-known solitons. Frequently, nonlinear periodic wave signals appear beside ion-acoustic soliton and double layer structures in auroral and magnetospheric plasmas [16]. Experimentally, cnoidal waves have been observed in water [17,18]. Moreover, cnoidal waves have been applied as a fundamental basis function to develop a new kind of nonlinear Fourier analysis to explain Adriatic Sea waves [19]. On the other side, Kauschke and Schlüter [20] explained single-mode drift wave spectra at the edge of the tokamak plasma in their previous experiment [21] on the basis of cnoidal waves. Kartashov *et al.* [22,23] reported, respectively, that in contradistinction with the case of localized solitons (where the spectrum of perturbations is discrete) for cnoidal waves, one has a band of possible increments at each energy flow, and, under the proper conditions of low- and high-energy flows, the two-dimensional cnoidal waves appear to be robust enough to be observable in experiments. Recently, Yuan *et al.* [24] demonstrated that, due to the interaction of the cnoidal wave with the solitary wave, phonons can be radiated, which destroys the cnoidal wave and finally results in a loss of stability of the solitary wave. However, the basic features (amplitude and width) of cnoidal waves in a dense relativistic degenerate magnetoplasma consisting of relativistic degenerate electrons and nondegenerate cold ions is still lacking. Therefore, the purpose of this article is to study the effects of plasma number density, ion cyclotron frequency, and direction cosines on the characteristics of cnoidal waves in compact interstellar objects (e.g., white dwarfs). We present our article in the following way. First, in Sec. II, the basic equations governing our plasma system are presented. Then, in Sec. III, the nonlinear modified Korteweg–de Vries (KdV) equation is derived, with appropriate boundary conditions, using the reductive perturbation technique. In Sec. IV, we solve the nonlinear modified KdV equation and write down exact analytic solutions for the cnoidal and solitary waves. Furthermore, specific features and nontrivial limits of these solutions are discussed. In Sec. V, the numerical plots of nonlinear ion-acoustic cnoidal and solitary waves in a Sagdeev potential and phase plane are presented. Moreover, the effects of the plasma number density, the ion cyclotron frequency, and the direction cosines on the basic features of ion-acoustic cnoidal waves are described. Finally, in Sec. VI, we present our main conclusions.

II. BASIC EQUATIONS

We consider the propagation of nonlinear ion-acoustic cnoidal and solitary waves in a three-dimensional plasma system, whose constituents are relativistic degenerate inertialess electrons and nondegenerate inertial cold ions. This degenerate plasma system is assumed to be immersed in an external static magnetic field ($\vec{B} = B_0\hat{e}_z$, where $\hat{e}_z$ is a unit vector in the z direction). At equilibrium, the charge neutrality condition requires that $Zn_i^{(0)} = n_e^{(0)}$, where $n_i^{(0)}$ and $n_e^{(0)}$ are the unperturbed number densities of ions and electrons, respectively. For simplicity, let us assume that $Z = 1$. The dynamic of the nonlinear electrostatic waves propagating in such a degenerate plasma system is governed by [11,25]

$$\frac{\partial n_i}{\partial t} + \nabla\cdot(n_i\vec{u}_i) = 0, \tag{1}$$

$$\frac{\partial \vec{u}_i}{\partial t} + (\vec{u}_i\cdot\nabla)\vec{u}_i = -\nabla\varphi + \Omega(\vec{u}_i\times\hat{e}_z), \tag{2}$$

$$\nabla\varphi - \frac{1}{n_e}\frac{P_{e0}}{n_e^{(0)}E_{fe}}\nabla P_{\mathrm{erd}} = 0, \tag{3}$$

and

$$\nabla^2\varphi = n_e - n_i. \tag{4}$$

Here, the variables n_i and n_e are, respectively, the densities of ions and electrons. $\vec{u}_i$ and φ are the ion flow velocity and the electrostatic potential, respectively. $\nabla = (\partial/\partial x,\partial/\partial y,\partial/\partial z)$, where x, y, and z are the space coordinates, and t is the time variable. The variables appearing in Eqs. (1)–(4) have been appropriately normalized: $n_i \to n_i/\ n_i^{(0)}$, $n_e \to n_e/\ n_e^{(0)}$, $u_{i(x,y,z)} \to u_{i(x,y,z)}/C_F$, $\varphi \to e\varphi/E_{fe}$, $t \to t\omega_{pi}$, and $\nabla \to \nabla\,\lambda_{Fi}$, where $C_F\ (=\sqrt{E_{fe}/m_i})$ is the ion-acoustic speed, $\omega_{pi}(=\sqrt{4\pi e^2\,n_i^{(0)}/m_i})$ is the ion plasma frequency, and $\lambda_{Fi}(=\sqrt{E_{fe}/4\pi e^2\,n_i^{(0)}})$ is the Debye radius. Moreover, $\Omega\,[=(eB_0/m_ic)/\omega_{pi}]$ is the ion cyclotron frequency, $E_{fe}\ [=m_ec^2(\gamma_e-1)]$ is the relativistic Fermi energy of the electron, where $\gamma_e\ [=(1+\mu_e^2)^{1/2}]$ is the relativistic factor with $\mu_e\ (=p_{Fe}/m_ec)$, which is the normalized relativistic parameter and p_{Fe} the momentum on the Fermi surface [12]. The relativistic degenerate pressure for electrons P_{erd} is given by [5,6,11]

$$P_{\mathrm{erd}} = \frac{\pi m_e^4c^5}{3h^3}\left[\mu_e\left(2\mu_e^2-3\right)\left(\mu_e^2+1\right)^{1/2} + 3\sinh^{-1}(\mu_e)\right], \tag{5}$$

Now, let us expand Eq. (5) around the unperturbed density of electrons $n_e^{(0)}$ using the Taylor series expansion: We obtain

$$P_{\mathrm{erd}} \cong P_{e0} + \frac{2E_{fe}}{3\gamma_{e0}}\delta n_e + \frac{\left(\mu_{e0}^2+2\right)}{9n_e^{(0)}\gamma_{e0}^3}\delta n_e^2, \tag{6}$$

where δn_e denotes the perturbed electron number densities, and $\gamma_{e0} = (1+\mu_{e0}^2)^{1/2}$ with $\mu_{e0}\,(=p_{e0}/m_ec)$ and $p_{e0} = p_{Fe} = (3n_e^{(0)}h^3/8\pi)^{1/3}$. Putting Eq. (6) into Eq. (3), one can express the electron momentum equation as

$$n_e\frac{\partial\varphi}{\partial z} = \alpha_e\frac{\partial\delta n_e}{\partial z} + \beta_e\frac{\partial\delta {n_e}^2}{\partial z}, \tag{7}$$

where $\alpha_e = \frac{2}{3\gamma_{e0}}$ and $\beta_e = \frac{(\mu_{e0}^2+2)}{9\gamma_{e0}^3}$. Furthermore, m_i (m_e) is the ion (electron) mass, e is the magnitude of the electric charge, and c is the speed of the light in vacuum.

III. DERIVATION OF THE NONLINEAR MODIFIED KdV EQUATION

In order to investigate the propagation of nonlinear periodic ion-acoustic and solitary waves in a dense relativistic degenerate magnetoplasma, we follow the reductive perturbation technique, which leads to a scaling of the independent variables through the stretched coordinates [26],

$$\xi = \epsilon^{1/2}(\ell_x x + \ell_y y + \ell_z z - U_0 t), \quad \tau = \epsilon^{3/2} t, \tag{8}$$

where ϵ is a smallness parameter measuring the weakness of the nonlinearity, U_0 is the phase velocity of the wave to be determined later, and ℓ_x, ℓ_y, and ℓ_z are the direction cosines of the wave vector $\vec{k}$ along the x, y, and z axes, respectively, so that $\ell_x^2 + \ell_y^2 + \ell_z^2 = 1$. Moreover, the physical perturbed quantities are expanded about their equilibrium values in a power series of ϵ as

$$n_{i,e} = 1 + \epsilon n_{i,e}^{(1)} + \epsilon^2 n_{i,e}^{(2)} + \epsilon^3 n_{i,e}^{(3)} + \cdots, \tag{9}$$

$$u_{i(x,y)} = \epsilon^{3/2} u_{i(x,y)}^{(1)} + \epsilon^2 u_{i(x,y)}^{(2)} + \cdots, \tag{10}$$

$$u_{i(z)} = \epsilon u_{i(z)}^{(1)} + \epsilon^2 u_{i(z)}^{(2)} + \epsilon^3 u_{i(z)}^{(3)} + \cdots, \tag{11}$$

$$\varphi = \epsilon \varphi^{(1)} + \epsilon^2 \varphi^{(2)} + \epsilon^3 \varphi^{(3)} + \cdots. \tag{12}$$

Substituting Eqs. (8)–(12) into the basic set of Eqs. (1)–(4) and (7), and equating terms with the same powers of ϵ, we obtain a set of equations for each order in ϵ. The set of equations at the lowest order, i.e.,

$$-U_0 \frac{\partial n_i^{(1)}}{\partial \xi} + \ell_z \frac{\partial u_{iz}^{(1)}}{\partial \xi} = 0, \tag{13a}$$

$$-\ell_x \frac{\partial \varphi^{(1)}}{\partial \xi} + \Omega u_{iy}^{(1)} = 0, \tag{13b}$$

$$\ell_y \frac{\partial \varphi^{(1)}}{\partial \xi} + \Omega u_{ix}^{(1)} = 0, \tag{14a}$$

$$-U_0 \frac{\partial u_i^{(1)}}{\partial \xi} + \ell_z \frac{\partial \varphi^{(1)}}{\partial \xi} = 0, \tag{14b}$$

$$n_i^{(1)} = n_e^{(1)}, \tag{15a}$$

$$-\alpha_e \frac{\partial n_e^{(1)}}{\partial \xi} + \frac{\partial \varphi^{(1)}}{\partial \xi} = 0, \tag{15b}$$

Moreover, after some algebraic manipulation, the following relations are obtained:

$$U_0 = \ell_z \sqrt{\alpha_e}, \tag{16a}$$

$$\mathrm{n}_i^{(1)} = \frac{\ell_z^2}{U_0^2} \varphi^{(1)} + C_1(\tau), \tag{16b}$$

$$u_{iz}^{(1)} = \frac{\ell_z}{U_0} \varphi^{(1)} + C_2(\tau), \tag{17a}$$

$$n_e^{(1)} = \frac{1}{\alpha_e} \varphi^{(1)} + C_3(\tau), \tag{17b}$$

where $C_1(\tau)$, $C_2(\tau)$, and $C_3(\tau)$ are integration constants which are independent of ξ and may depend on the variable τ.

Now taking next higher-order equations,

$$-U_0 \frac{\partial n_i^{(2)}}{\partial \xi} + \frac{\partial n_i^{(1)}}{\partial \tau} + \ell_z \frac{\partial \left(n_i^{(1)} u_{iz}^{(1)}\right)}{\partial \xi} + \ell_x \frac{\partial u_{ix}^{(2)}}{\partial \xi} + \ell_y \frac{\partial u_{iy}^{(2)}}{\partial \xi} + \ell_z \frac{\partial u_{iz}^{(2)}}{\partial \xi} = 0, \tag{18}$$

$$\frac{\partial u_{iz}^{(1)}}{\partial \tau} - U_0 \frac{\partial u_{iz}^{(2)}}{\partial \xi} + \ell_z \frac{\partial \left(n_i^{(1)} u_{iz}^{(1)}\right)}{\partial \xi} + \ell_z u_{iz}^{(1)} \frac{\partial u_{iz}^{(1)}}{\partial \xi} + \ell_z \frac{\partial \varphi^{(2)}}{\partial \xi} = 0, \tag{19}$$

$$u_{iy}^{(2)} = -\frac{U_0}{\Omega} \frac{\partial u_{ix}^{(1)}}{\partial \xi}, \tag{20a}$$

$$u_{ix}^{(2)} = \frac{U_0}{\Omega} \frac{\partial u_{iy}^{(1)}}{\partial \xi}, \tag{20b}$$

$$n_e^{(1)} \frac{\partial \varphi^{(1)}}{\partial \xi} + \frac{\partial \varphi^{(2)}}{\partial \xi} - \alpha_e \frac{\partial n_e^{(2)}}{\partial \xi} - \beta_e \frac{\partial n_e^{(1)2}}{\partial \xi} = 0, \tag{21}$$

$$\frac{\partial^2 \varphi^{(1)}}{\partial \xi^2} = n_e^{(2)} - n_i^{(2)}. \tag{22}$$

Furthermore, after some algebraic steps, with the aid of Eqs. (16) and (17), we obtain

$$\frac{\partial n_i^{(2)}}{\partial \xi} = \frac{2\ell_z^3}{U_0^2} \frac{\partial \varphi^{(1)}}{\partial \tau} + \frac{3\ell_z^4}{U_0^4} \varphi^{(1)} \frac{\partial \varphi^{(1)}}{\partial \xi} + \frac{\ell_z^2}{U_0^2} (C_1(\tau) + 2C_2(\tau)) \frac{\partial \varphi^{(1)}}{\partial \xi} + \frac{\left(1 - \ell_z^2\right)}{\Omega^2} \frac{\partial^3 \varphi^{(1)}}{\partial \xi^3} + \frac{\ell_z^2}{U_0^2} \frac{\partial \varphi^{(2)}}{\partial \xi} + \frac{1}{U_0} \frac{\partial C_1(\tau)}{\partial \tau} + \frac{\ell_z}{U_0} \frac{\partial C_2(\tau)}{\partial \tau}. \tag{23}$$

In the derivation of Eq. (23), the periodic boundary condition implies that

$$\frac{\partial C_1(\tau)}{\partial \tau} = \frac{\partial C_2(\tau)}{\partial \tau} = 0. \tag{24}$$

Therefore, C_1 and C_2 are independent of ξ and τ. It should be mentioned here that, from Eq. (15a), C_1 is equal to C_3. Thus, C_1, C_2, and C_3 are just constants. Accordingly, we can express $\frac{\partial n_i^{(2)}}{\partial \xi}$ and $\frac{\partial n_e^{(2)}}{\partial \xi}$ as

$$\frac{\partial n_i^{(2)}}{\partial \xi} = \frac{2\ell_z^3}{U_0^2} \frac{\partial \varphi^{(1)}}{\partial \tau} + \frac{3\ell_z^4}{U_0^4} \varphi^{(1)} \frac{\partial \varphi^{(1)}}{\partial \xi} + \frac{\ell_z^2}{U_0^2} (C_1 + 2C_2) \frac{\partial \varphi^{(1)}}{\partial \xi} + \frac{\left(1 - \ell_z^2\right)}{\Omega^2} \frac{\partial^3 \varphi^{(1)}}{\partial \xi^3} + \frac{\ell_z^2}{U_0^2} \frac{\partial \varphi^{(2)}}{\partial \xi}, \tag{25}$$

$$\frac{\partial n_e^{(2)}}{\partial \xi} = \frac{1}{\alpha_e^3} (\alpha_e - 2\beta_e) \varphi^{(1)} \frac{\partial \varphi^{(1)}}{\partial \xi} + \frac{C_1}{\alpha_e^2} (\alpha_e - 2\beta_e) \frac{\partial \varphi^{(1)}}{\partial \xi} + \frac{1}{\alpha_e} \frac{\partial \varphi^{(2)}}{\partial \xi}. \tag{26}$$

After differentiating Eq. (22) and using Eqs. (25) and (26), we have the nonlinear modified KdV equation for describing the nonlinear dynamics of ion-acoustic cnoidal and solitary waves in the presence of nondegenerate inertial cold ions and the relativistic degenerate inertialess electrons in magnetized plasmas as follows:

$$\frac{\partial \varphi^{(1)}}{\partial \tau} + A\varphi^{(1)}\frac{\partial \varphi^{(1)}}{\partial \xi} + B\frac{\partial^3 \varphi^{(1)}}{\partial \xi^3} + C\frac{\partial \varphi^{(1)}}{\partial \xi} = 0, \quad (27)$$

where

$$A = \frac{U_0}{\alpha_e^2}(\alpha_e + \beta_e), \quad B = \frac{U_0 \alpha_e}{2}\left(1 + \frac{(1-\ell_z^2)}{\Omega^2}\right),$$
$$C = \frac{U_0}{\alpha_e}\left(\frac{U_0 C_1}{\ell_z} + \beta_e C_2\right).$$

IV. CNOIDAL WAVE-SOLITON SOLUTION OF THE NONLINEAR MODIFIED KdV EQUATION

Now, let us find the explicit stationary solutions of Eq. (27): We introduce $\zeta = \xi - U_1\tau$, where U_1 is the velocity of the nonlinear structure moving with the frame. By transforming Eq. (27) into the ζ coordinate, after some algebraic steps, we will obtain the energy conservation law as follows:

$$\frac{1}{2}\left(\frac{\partial \Phi}{\partial \zeta}\right)^2 + V(\Phi) = 0, \quad (28a)$$

where the Sagdeev potential $V(\Phi)$ is given by

$$V(\Phi) = \frac{A}{6B}\Phi^3 - \frac{U}{2B}\Phi^2 + \rho_0\Phi - \frac{1}{2}E_0^2, \quad (28b)$$

where $\frac{1}{2}E_0^2$ is the integration constant having the meaning of the total energy of oscillations, $U = U_1 - C$, and $\varphi^{(1)} = \Phi$. In addition, ρ_0 and E_0 are the charge density and the electric field when the potential Φ vanishes. Therefore, one can define E_0^2 by using the following initial conditions $\Phi(0) = \phi_0$ and $d\Phi(0)/d\zeta = 0$:

$$E_0^2 = \frac{A}{3B}\phi_0^3 - \frac{U}{B}\phi_0^2 + 2\rho_0\phi_0. \quad (29)$$

Substituting Eq. (29) into Eq. (28), after some algebraic manipulations, we have

$$\left(\frac{\partial \Phi}{\partial \zeta}\right)^2 = \frac{A}{3B}(\phi_0 - \Phi)(\Phi - \phi_1)(\Phi - \phi_2), \quad (30)$$

where $\phi_{1,2} = \frac{3}{2}[\frac{U}{A} - \frac{\phi_0}{3} \pm \sqrt{\frac{1}{3}(\Psi_1 - \phi_0)(\phi_0 - \Psi_2)}]$ and $\Psi_{1,2} = \frac{U}{A} \pm 2\sqrt{\frac{U^2}{A^2} - 2\rho_0\frac{B}{A}}$.

The last relations indicate that the inequality $\Psi_2 \leqslant \phi_0 \leqslant \Psi_1$, or $\Psi_1 \leqslant \phi_0 \leqslant \Psi_2$, should be satisfied. Moreover, the following relation can be obtained from Eqs. (28) and (30):

$$U = \frac{A}{3}(\phi_0 + \phi_1 + \phi_2). \quad (31)$$

The periodic wave solution of Eq. (28) is given by [27,28]

$$\Phi(\zeta) = \phi_1 + \psi_{\text{cn}}\,\text{cn}^2(D\zeta, m), \quad (32)$$

where cn is the Jacobian elliptic function, whereas the parameters m ($0 < m < 1$) and D are defined as

$$m^2 = \frac{(\phi_0 - \phi_1)}{(\phi_0 - \phi_2)}, \quad (33)$$

$$D = \sqrt{\frac{A}{12B}(\phi_0 - \phi_2)}. \quad (34)$$

Physically, the elliptic parameter m (the modulus) may be viewed as a fair indicator of the nonlinearity with the linear limit being $m \to 0$ and the extreme nonlinear limit being $m \to 1$. The conditions for the existence of a cnoidal solution of Eq. (32) require that $\phi_0 > \phi_1 \geqslant \phi_2$ and $\phi_1 \leqslant \Phi \leqslant \phi_0$. Furthermore, the amplitude ψ_{cn}, the wavelength λ, and the frequency ν of the cnoidal wave are defined as

$$\psi_{\text{cn}} = (\phi_0 - \phi_1), \quad (35)$$

$$\lambda = 4\sqrt{\frac{3B}{A(\phi_0 - \phi_2)}}\,\text{K}(m), \quad (36)$$

$$\nu = V/\lambda, \quad (37)$$

where K(m) is the first kind of complete elliptic integral and V ($=U_0 + U_1$) is the velocity of the cnoidal waves in the laboratory frame.

Now, let us describe the soliton solution for two limits. For the first case, $m \to 1$, $\rho_0 \neq 0$, and $E_0 \neq 0$, this case can be achieved at $\phi_0 \approx \Psi_1$ or $\phi_0 \approx \Psi_2$. On doing this, we arrive at the following relation:

$$\phi_1 \approx \phi_2 = \frac{U}{A} \pm \sqrt{\left(\frac{U}{A}\right)^2 - 2\rho_0\frac{B}{A}}. \quad (38)$$

Therefore, K(m) $\to \infty$ and the Jacobi elliptic function cn δ degenerates to the hyperbolic function sech δ, (i.e., cn $\delta \to$ sech δ) [29–31]. Consequently, the wavelength λ [i.e., Eq. (36)] tends to infinity and the periodic solution [i.e., Eq. (32)] becomes the soliton solution,

$$\Phi(\zeta) = \phi_1 + (\phi_0 - \phi_1)\text{sech}^2\left(\sqrt{\frac{A}{12B}(\phi_0 - \phi_1)}\zeta\right). \quad (39)$$

Clearly, Eq. (39) indicates that ϕ_1 represents the potential at $\zeta \to \pm\infty$. On the other side, the second case ($m \to 1$ and $\rho_0 = E_0 = 0$) can be realized at $\phi_1 = \phi_2 = 0$. In this case, $\psi_{\text{cn}} = \phi_0 = 3U_1/A = \psi_m$, $D = \sqrt{A\phi_0/12B} = \sqrt{U_1/4B} = 1/W$, and cn $\delta \to$ sech δ [29–31], then the cnoidal wave solution [i.e., Eq. (32)] is reduced to the ion-acoustic soliton solution

$$\Phi(\zeta) = \psi_m\,\text{sech}^2(\zeta/W), \quad (40)$$

where ψ_m($=3U_1/A$) and W ($=\sqrt{4B/U_1}$) are the amplitude and the width of the ion-acoustic solitary wave, respectively.

V. NUMERICAL RESULTS AND DISCUSSIONS

In the preceding section, we have introduced an analytical description for the propagation of ion-acoustic cnoidal and solitary waves in a dense relativistic degenerate magnetoplasma consisting of relativistic degenerate electrons and nondegenerate cold ions using the solutions [Eq. (32) of cnoidal waves, Eqs. (39) and (40) of solitary waves, of the derived Eq. (27) "nonlinear modified KdV equation"]. However, before proceeding to the nonlinear analysis, it is interesting to examine the polarity of the nonlinear structures. As is evident from the nonlinear modified KdV equation, the nonlinear coefficient A and the dispersion coefficient B are always positive. Therefore, in our system under consideration, only compressive (i.e., hump) structures of the nonlinear periodic and solitary waves are formed. Here, we try to analyze our results numerically. For illustration, parameters are chosen that are representative of the relativistic plasmas found in white dwarfs. Consider $n_e^{(0)} \approx 10^{30}$–$10^{31}$ cm^3 and $B_0 \approx 10^{10}$ G [11]. Figure 1 represents the variation in the Sagdeev potential $V(\Phi)$ with respect to potential Φ using Eq. (28). Clearly, the solid (the dashed) curve in Fig. 1 demonstrates the Sagdeev potential $V(\Phi)$ corresponding to the cnoidal wave (solitary wave). In the case of a cnoidal wave (i.e., $\rho_0 \neq 0$ and $E_0 \neq 0$), the three real zeros of the Sagdeev potential corresponding to the cnoidal wave are ϕ_0, ϕ_1, and ϕ_2. Furthermore, the Sagdeev potential corresponding to the cnoidal wave does not become zero at $\Phi = 0$. In addition, physically, one can observe that this Sagdeev potential is such that the pseudoparticle oscillates periodically back and forth in the potential well between points ϕ_0 and ϕ_1 and cannot reach point ϕ_2 due to the small potential barrier. Accordingly, the potential structure corresponding to the cnoidal wave is repeated and the distance between repetitions of the wave shape corresponds to one wavelength. On the other hand, in the case of a soliton (i.e., $\rho_0 = E_0 = 0$), the Sagdeev potential $V(\Phi)$ becomes zero at $\Phi = 0$. To support the results displayed in Fig. 1, we have also made a corresponding phase plane for the ion-acoustic cnoidal wave (bounded solid curve) and the soliton described by a separatrix (dashed curve). The numerical results are displayed in Fig. 2, where we have plotted the phase plane for the fixed

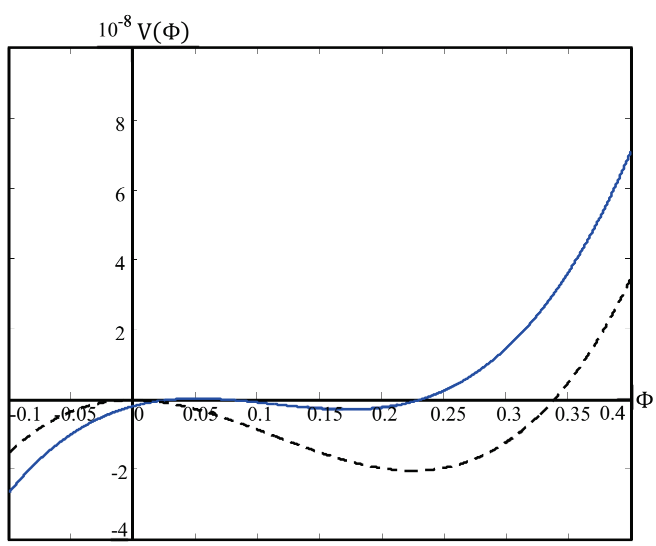

FIG. 1. (Color online) Variation in Sagdeev potential $V(\Phi)$ with respect to the potential Φ using Eq. (28), for $n_e^{(0)} = 1 \times 10^{31}$, $\ell_z = 0.6$, $\Omega = 0.0006$, $U = 0.15$, and $(|E_0|,\rho_0) = (0.000\,07, 1 \times 10^{-7})$ (solid curve) and (0,0) (dashed curve).

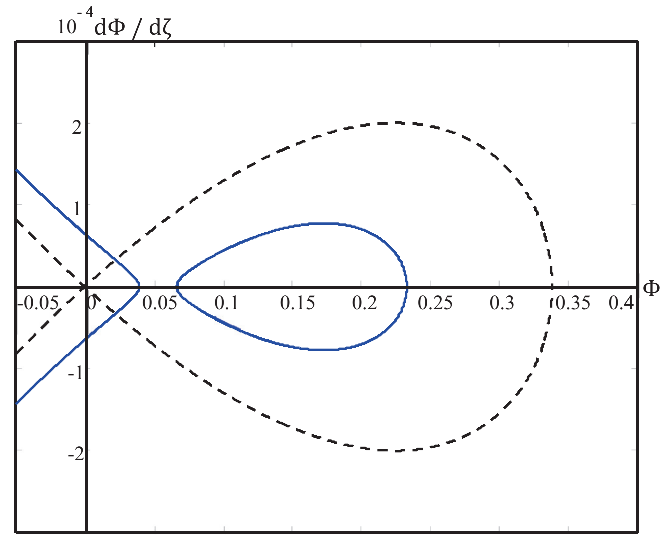

FIG. 2. (Color online) Phase curves using Eqs. (28) and (30), with $n_e^{(0)} = 1 \times 10^{31}$, $\ell_z = 0.6$, $\Omega = 0.0006$, $U = 0.15$, and $(|E_0|,\rho_0) = (0.000\,07, 1 \times 10^{-7})$ (solid curve) and (0,0) (dashed curve).

values of the parameters as taken in Fig. 1. In the solid phase plane (i.e., $\rho_0 \neq 0$ and $E_0 \neq 0$) of Fig. 2, one can note that the phase curve is repeated on the same path and one complete cycle corresponds to a wavelength in the physical space. This means, physically, that whenever the pseudoparticle's velocity becomes zero [i.e., $(d\Phi/d\zeta = 0)$], the potential force reflects it back [since $-dV(\Phi)/d\Phi \neq 0$], and then it oscillates between two points ϕ_0 and ϕ_1. Therefore, the closed curve in the phase plane implies that the trajectory is a periodic orbit. On the other side, the dashed phase curve (i.e., $\rho_0 = E_0 = 0$) in Fig. 2 emerges from the origin, circling anticlockwise around the positive Φ axis, and again stops at the origin, entering from the upper side. In the mechanical analogy, at $\Phi = 0$, the pseudoparticle starts with zero speed and gains some speed along the positive Φ axis. After getting maximum speed, its speed decreases and becomes zero at $\Phi = \Phi_{\rm max}$. Furthermore, due to a potential force, the pseudoparticle bounces back toward the origin, which acts on it, where $-dV(\Phi)/d\Phi \neq 0$, gains speed in the opposite direction (i.e., along the negative Φ axis), and returns to rest at position $\Phi = 0$. In physical space, the electric potential Φ increases from zero (at $\zeta = -\infty$), attains a maximum value at $\Phi = 0$, and then decreases until it becomes zero (at $\zeta = \infty$). This potential structure does not repeat and it represents an ion-acoustic soliton [26]. Figure 3 demonstrates the profiles of the cnoidal wave [i.e., Eq. (32)], the solitary wave [using the solution of Eq. (39)], and the soliton solution of Eq. (40). Furthermore, Fig. 3 illustrates how the cnoidal wave shrinks, under certain conditions, to the solitary wave. It should be mentioned here that the soliton solution of Eq. (40) completely agrees with the recent work of Rahman *et al.* [11].

Numerically, for example, let us consider $n_e^{(0)} = 10^{31}$ cm^3, $B_0 = 10^{10}$ G, and $\ell_z = 0.7$: The characteristic plasma parameters become U_0 (the phase velocity)= 0.4915, ψ_m (the solitary wave amplitude) = 0.1772, and W (the width of the ion-acoustic solitary wave) = 40 047, which are in agreement

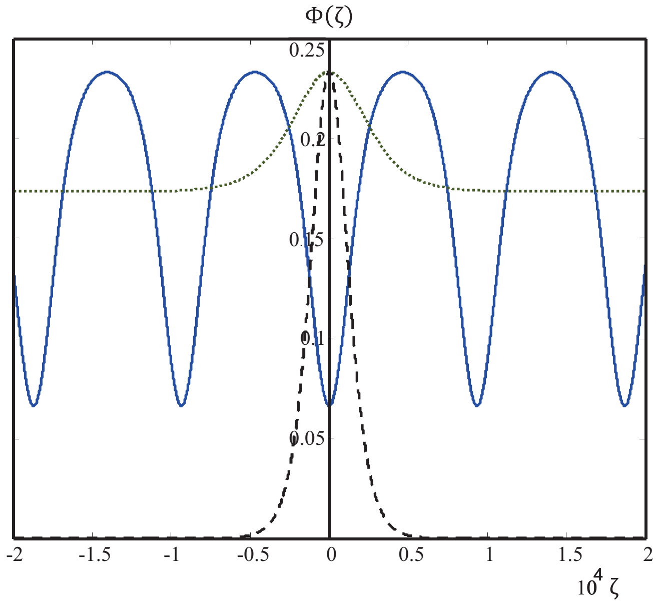

FIG. 3. (Color online) Variation in Φ with respect to ζ, $n_e^{(0)} = 1 \times 10^{31}$, $\ell_z = 0.6$, $\Omega = 0.0006$, and $(|E_0|,\rho_0) = (0.000\,07, 1 \times 10^{-7})$ (solid curve, ion-acoustic cnoidal wave), using Eq. (32), $(0.000\,07, 1 \times 10^{-7})$ (dotted curve, ion-acoustic solitary wave), using Eq. (39), and (0,0) (dashed curve, ion-acoustic solitary wave), using Eq. (40).

with the numerical values of Rahman *et al.* [11]. Here, we will now investigate the effects of plasma number density $n_e^{(0)}$, ion cyclotron frequency Ω, and direction cosines ℓ_z on the basic properties of ion-acoustic cnoidal waves. The results are displayed in Figs. 4–6. In Fig. 4, the effect of plasma number density on the profile of the ion-acoustic cnoidal waves against the space coordinate ζ is investigated. It is clear

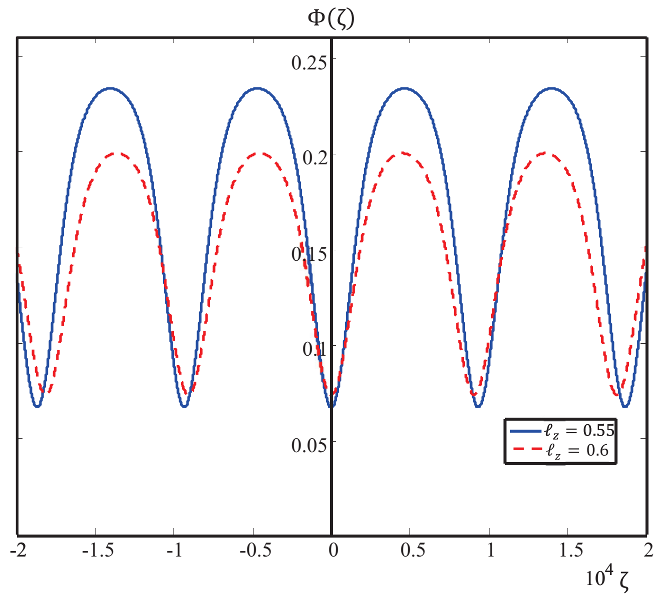

FIG. 5. (Color online) Variation of ion-acoustic cnoidal wave Φ with respect to ζ, $n_e^{(0)} = 1 \times 10^{31}$, $\Omega = 0.0006$, $U = 0.15$, $(|E_0|,\rho_0) = (0.000\,07, 1 \times 10^{-7})$, $\ell_z = 0.55$ (solid curve), and $\ell_z = 0.6$ (dashed curve).

that the amplitude and the width of the cnoidal wave grow up due to the increase of plasma number density $n_e^{(0)}$. This behavior arises due to the fact that the restoring force of the ion-acoustic cnoidal wave is provided by electron pressure, and that increasing $n_e^{(0)}$ can be viewed as an equivalent process for increasing electron pressure, which, in turn, makes the amplitude of the ion-acoustic cnoidal wave higher. On the other hand, the increase of $n_e^{(0)}$ causes the coefficient of the dispersion term in the nonlinear modified KdV equation to

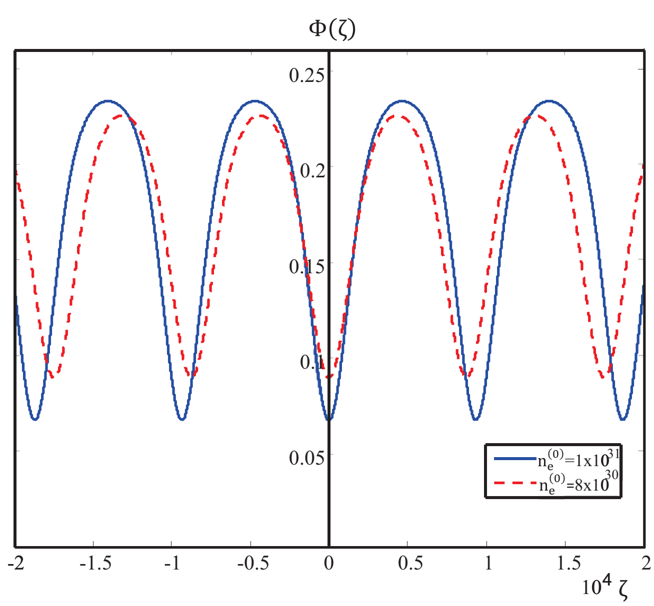

FIG. 4. (Color online) Variation of ion-acoustic cnoidal wave Φ with respect to ζ, $\ell_z = 0.6$, $\Omega = 0.0006$, $U = 0.15$, $(|E_0|,\rho_0) = (0.000\,07, 1 \times 10^{-7})$, $n_e^{(0)} = 1 \times 10^{31}$ (solid curve), and $n_e^{(0)} = 8 \times 10^{30}$ (dashed curve).

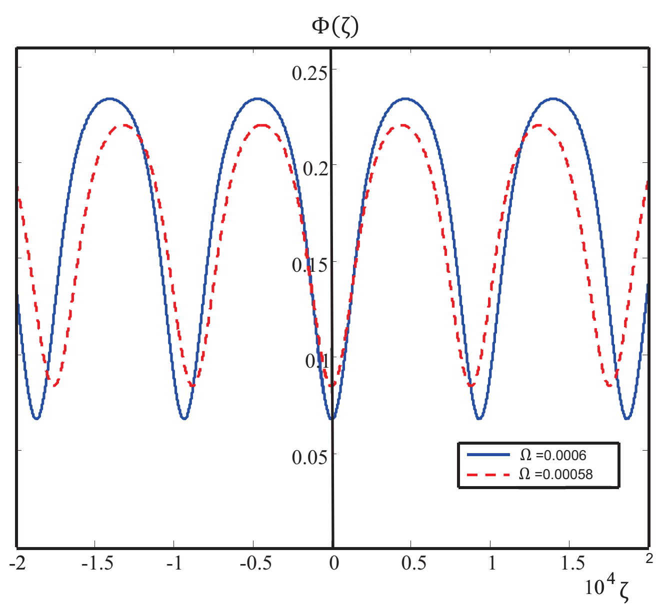

FIG. 6. (Color online) Variation of ion-acoustic cnoidal wave Φ with respect to ζ, $n_e^{(0)} = 1 \times 10^{31}$, $\ell_z = 0.6$, $U = 0.15$, $(|E_0|,\rho_0) = (0.000\,07, 1 \times 10^{-7})$, $\Omega = 0.0006$ (solid curve), and $\Omega = 0.000\,58$ (dashed curve).

be smaller, and, as a result, the cnoidal wave becomes fatter. In Fig. 5, the variation of the profile of the ion-acoustic cnoidal wave with ℓ_z (the direction cosines of the wave vector $\vec{k}$ along the z axis) is examined. It is manifest that both the amplitude and the width increase as ℓ_z decreases. It can be predicted that as the cnoidal wave approaches the direction perpendicular to the magnetic field, the amplitude and the width of the cnoidal wave would become extremely large, and from this point, the cnoidal wave disappears. Now, let us look at the effect of ion cyclotron frequency Ω on the ion-acoustic cnoidal wave which is exhibited in Fig. 6. It is seen that the amplitude and the width of the cnoidal wave increase as Ω increases. It means that for an increase of B_0 (the external static magnetic field), the coefficient of the dispersion term in the nonlinear modified KdV equation is smaller, which in turn leads, respectively, to the increase (decrease) of the numerical value of $\phi_0(\phi_1)$, and consequently, the amplitude and the width of the cnoidal wave go up.

VI. CONCLUSION

This article considered a three-dimensional dense relativistic degenerate magnetoplasma system composed of relativistic degenerate electrons and nondegenerate cold ions. The nonlinear propagation of the cnoidal and solitary waves is described by a nonlinear modified KdV equation. The compressive structures of the allowed ion-acoustic cnoidal and solitary waves are formed. In the particular case of a soliton [11], this is in agreement with what has been observed in the dense relativistic degenerate magnetoplasma model [11], which reveals compressive solitons only. Under nontrivial limits of the cnoidal wave solution, we deduced exact analytic solutions for the soliton solutions. Furthermore, the effects of plasma number density, ion cyclotron frequency, and direction cosines on the profile of ion-acoustic cnoidal waves are discussed and graphically displayed. It is found that the amplitude and the width of the cnoidal wave enhance (diminish) due to the increase of plasma number density and ion cyclotron frequency (the direction cosines of the wave vector $\vec{k}$ along the z axis). The present findings show significant modifications of the basic properties of the cnoidal wave solutions (amplitude and width) and reveal different features in comparison with a recent study of solitary waves in the dense relativistic degenerate case [11]. Moreover, the behavior of ion-acoustic cnoidal waves is completely different from the behavior of ion-acoustic solitary waves. It is hoped that ion-acoustic cnoidal waves can be really observed in dense relativistic degenerate plasmas. Moreover, the cnoidal wave and soliton solutions obtained in this article may have applications in certain astrophysical scenarios, especially dense plasmas in the atmosphere of neutron stars and the interior of massive white dwarfs [32].

ACKNOWLEDGMENTS

The author would like to express his gratitude to the referee for a number of valuable criticisms and comments that have led to improvement of the original manuscript. The author also thanks the editor and his staff for their kind cooperation.

[1] G. Manfredi and F. Haas, Phys. Rev. B **64**, 075316 (2001).
[2] P. K. Shukla, Phys. Lett. A **352**, 242 (2006).
[3] A. Ghoshal and Y. K. Ho, Phys. Rev. E **81**, 016403 (2010).
[4] E. F. El-Shamy and F. S. Gohman, Phys. Lett. A **378**, 2688 (2014).
[5] S. Chandrasekhar, Astrophys. J. **74**, 81 (1931).
[6] S. Chandrasekhar, Philos. Mag. **11**, 592 (1931).
[7] S. Chandrasekhar, Mon. Not. R. Astron. Soc. **170**, 405 (1935).
[8] S. L. Shapiro and S. A. Teukolsky, *Black Holes, White Dwarfs, and Neutron Stars: The Physics of Compact Objects* (Wiley, New York, 1983).
[9] E. Garcia-Berro, S. Torres, L. G. Althaus, I. Renedo, P. Lorén-Aguilar, A. H. Córsico, R. D. Rohrmann, M. Salaris, and J. Isern, Nature (London) **465**, 194 (2010).
[10] W. F. El-Taibany and A. A. Mamun, Phys. Rev. E **85**, 026406 (2012).
[11] A. Rahman, W. Masood, B. Eliasson, and A. Qamar, Phys. Plasmas **20**, 092305 (2013).
[12] D. E. Winget and S. O. Kepler, Annu. Rev. Astron. Astrophys. **46**, 157 (2008).
[13] G. Fontaine and P. Brassard, Publ. Astron. Soc. Pac. **120**, 1043 (2008).
[14] J. P. Ostriker, Annu. Rev. Astron. Astrophys. **9**, 353 (1971).
[15] B. Eliasson and P. K. Shukla, Europhys. Lett. **97**, 15001 (2012).
[16] A. V. Gurevich and L. Stenflo, Phys. Scr. **38**, 855 (1988).
[17] W. J. Pierson, Jr., M. A. Donelan, and W. H. Hui, J. Geophys. Res. **97**, 5607 (1992).
[18] D. Rubensteain, IEEE J. Oceanic Eng. **24**, 346 (1999).
[19] A. R. Osborne, M. Serio, L. Bergamasco, and L. Cavaleri, Physica D **123**, 64 (1998).
[20] U. Kauschke and H. Schlüter, Plasma Phys. Controlled Fusion **33**, 1309 (1991).
[21] U. Kauschke and H. Schlüter, Plasma Phys. Controlled Fusion **32**, 1149 (1990).
[22] Y. V. Kartashov, V. A. Vysloukh, and L. Torner, Phys. Rev. E **67**, 066612 (2003).
[23] Y. V. Kartashov, V. A. Vysloukh, and L. Torner, Phys. Rev. E **68**, 015603(R) (2003).
[24] Z. Yuan, J. Wang, M. Chu, G. Xia, and Z. Zheng, Phys. Rev. E **88**, 042901 (2013).
[25] A. Rasheed, G. Murtaza, and N. L. Tsintsadze, Phys. Rev. E **82**, 016403 (2010).
[26] L. L. Yadav and V. K. Sayal, Phys. Plasmas **16**, 113703 (2009).
[27] V. I. Karpman, *Nonlinear Waves in Dispersive Media* (Pergamon, Oxford, UK, 1975).
[28] T. Kaladze and S. Mahmood, Phys. Plasmas **21**, 032306 (2014).
[29] M. Abramowitz and I. A. Stegun, *Handbook of Mathematical Functions* (Dover, New York, 1972).
[30] V. Prasolov and Y. Solovyev, *Elliptic Functions and Elliptic Integral* (American Mathematical Society, Providence, RI, 1977).
[31] Y.-Z. Peng, Phys. Lett. A **337**, 55 (2005).
[32] A. J. Keane, A. Mushtaq, and M. S. Wheatland, Phys. Rev. E **83**, 066407 (2011).